

MODIFIED COMPRESSIVE SENSING FOR REAL-TIME DYNAMIC MR IMAGING

Wei Lu and Namrata Vaswani

Department of Electrical and Computer Engineering, Iowa State University
{luwei,namrata}@iastate.edu

ABSTRACT

In this work, we propose algorithms to recursively and causally reconstruct a sequence of natural images from a reduced number of linear projection measurements taken in a domain that is “incoherent” with respect to the image’s sparsity basis (typically wavelet) and demonstrate their application in real-time MR image reconstruction. For a static version of the above problem, Compressed Sensing (CS) provides a provably exact and computationally efficient solution. But most existing solutions for the actual problem are either offline and non-causal or cannot compute an exact reconstruction (for truly sparse signal sequences), except using as many measurements as those needed for CS. The key idea of our proposed solution (modified-CS) is to design a modification of CS when a part of the support set is known (available from reconstructing the previous image). We demonstrate the exact reconstruction property of modified-CS on full-size image sequences using much fewer measurements than those required for CS. Greatly improved performance over existing work is demonstrated for approximately sparse signals or noisy measurements.

Index Terms— Modified compressive sensing

1. INTRODUCTION

In this work, we propose algorithms to recursively and causally reconstruct a sequence of natural images from a reduced number of linear projection measurements taken in a domain that is “incoherent” with respect to the image’s sparsity basis (typically wavelet) and demonstrate their application in real-time MR image reconstruction. Natural images, e.g., cross-sectional images of human organs, e.g. heart or brain, are usually piecewise smooth and thus (approximately) sparse in the wavelet transform domain. This fact forms the basis of JPEG2000. An approximate model for such images is to assume that the image’s wavelet transform is a sparse vector, i.e. only a small number of its elements are nonzero, the rest are exactly zero. The set of indices of the (significantly) nonzero coefficients (the “sparsity pattern” or the “support set”) is not known a-priori and changes with time. In a time sequence of such signals, due to temporal dependencies, it is empirically observed that the *sparsity pattern changes very slowly with time*, See Fig. 1. MRI measures the 2D discrete Fourier transform (DFT) of the image, which is known to be incoherent w.r.t. the wavelet basis. MR scanning is sequential and hence there is always a need to reduce the number of measurements required for high-fidelity reconstruction. The ability to reconstruct in real-time is critical to making “interventional MR” applications, such as MR-guided neurosurgery, practical [10].

Since the introduction of compressive sensing (CS) [3, 7] the static version of the above problem has been thoroughly studied. But, with the exception of [13, 8], most existing solutions for the time

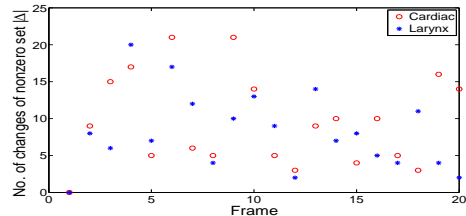


Fig. 1. Slow change in sparsity pattern of the wavelet coefficients (2-level Daubechies-4 wavelets). The size of the 99% energy support set varied between 4400 - 4600 (less than 7% of all coefficients) for the larynx sequence and between 1400 - 1500 (less than 9% of all coefficients) for the cardiac sequence. As can be seen, the maximum size of the change is 20 for larynx and 22 for cardiac, i.e. less than 2% of the minimum sparsity size in both cases.

series problem are non-causal or batch solutions with very high complexity. The alternative solution - separately doing CS at each time (simple CS) - is causal and low complexity, but requires many more measurements for accurate reconstruction. In recent work [14, 12], we studied the causal reconstruction problem from noisy measurements and proposed a solution called Kalman filtered CS(KF-CS) and its non-Bayesian version, least squares CS(LS-CS). The reason LS-CS(KF-CS), significantly outperformed simple CS was that the signal minus its LS(KF) estimate (computed using the previous support estimate) contains much fewer significantly nonzero elements than the signal itself. But its exact sparsity size (total number of nonzero coefficients) is equal to or larger than that of the signal and the number of measurements required for exact reconstruction is governed by the exact sparsity size, one thing we were not able to achieve was exact reconstruction using fewer (noiseless) measurements than those needed by simple CS.

The key idea of our proposed solution (modified-CS) is to design a modification of CS when a part of the support set is known. In this work we assume that this is the estimated support of the wavelet coefficients’ vector of the previous image. We introduced the main idea of modified-CS for noiseless measurements in [11] and proved that, for truly sparse signal/image sequences, it can achieve exact reconstruction using *much fewer* noiseless measurements than simple CS. To our knowledge, *there is no other existing work that demonstrates or proves exact reconstruction for CS with partly known support using much fewer measurements than those needed by CS*. The works of [13, 8, 6] use different methods to reconstruct a difference image (current image minus its prediction). Doing this will work better than simple CS only if the exact sparsity size of the difference image is small compared to that of the current image and the sparsity basis of the difference image is known. This does not usually hold.

We begin by repeating the modified-CS algorithm for noiseless measurements and then we introduce its modification for noisy measurements in Sec. 3. Since we only had results on toy problems

This work is supported by NSF grants ECCS-0725849 and CCF-0917015.

with image sizes less than 64×64 because we were using standard linear programming software in which the interior solver needs to be specified using matrices. The maximum input matrix size is limited by the maximum memory of the PC (or actually of MATLAB). Even for a 64×64 image, the code ran very slowly because it was using almost all the RAM of the PC. In this work, we demonstrate superior performance of modified-CS for full size MRI reconstruction using “operator version”, see Fig. 3 and 4. The details are given in Sec. 4. The operator version also results in a significant algorithm speedup, primarily because of fast 2D implementations of discrete Fourier and wavelet transforms replacing the matrix version. In Sec. 5, we compare our method against LS-CS.

1.1. Problem Definition

The problem definition is similar to [12]. For an image sequence, let $(Z_t)_{m_1 \times m_1}$ denote the image at time t and let $m := m_1^2$ be its dimension. Let X_t denote the 2D discrete wavelet transform (DWT) of Z_t , i.e. $X_t := WZ_tW'$, where W is the DWT matrix. Let $Y_{full,t} = FZ_tF = FW'X_tWF$ be the 2D discrete Fourier transform (DFT) of Z_t . Here F is the DFT matrix. The above can be transformed to a 1D problem by using Kronecker product, denoted by \otimes . Let $y_{full,t} := \text{vec}(Y_{full,t})$ and $x_t := \text{vec}(X_t)$. Here, $\text{vec}(X_t)$ denotes the vectorization of the matrix X_t formed by stacking the columns of X_t into a single column vector. Then $y_{full,t} = F_{1D}W'_{1D}x_t$ where $F_{1D} = F \otimes F$ and $W'_{1D} = W' \otimes W'$.

In MRI, we capture a smaller number, $n < m$, of Fourier coefficients of the image. This can be modeled by applying an $n \times m$ mask, M (which contains a single 1 at a different location in each row and all other entries are zero) to $y_{full,t}$ to get the observation y_t . The above can be rewritten as

$$y_t = Ax_t, \text{ where } A := H\Phi, \quad (1)$$

and $H := MF_{1D}$ and $\Phi := W'_{1D}$. The measurement matrix, A , is “approximately orthonormal” for sub-matrices containing $S = (|T| + 2|\Delta|)$ or less columns [11]. In certain situations, the MR measurements are noisy. This can be modeled as

$$y_t = Ax_t + w_t, \quad w_t \sim \mathcal{N}(0, \sigma_{obs}^2 I) \quad (2)$$

Notation: We use $'$ for transpose. The notation $\|x\|_k$ denotes the ℓ_k norm of the vector x . A_T is to denote the sub-matrix containing the columns of A with indices belonging to T . For a vector, the notation $(x)_T$ forms a sub-vector that contains elements with indices in T . Let N_t denote the current set of nonzero coefficients (significantly nonzero coefficients in case of compressible sequences) of x_t . For $(x_t)_{N_t}$, we assume that the set, N_t , of (significantly) nonzero coefficients of x_t change slowly over time. For example, wavelet coefficients of real image sequences are compressible. In this case, we use “support” to denote the smallest set containing enough wavelet coefficients so that their energy is equal to 99% of the total image energy. For a 128×128 cardiac image, we observed that $|N_t| \approx 1500$, but $|\Delta_t| = |N_t \setminus N_{t-1}| \leq 40$.

2. MODIFIED-CS FOR NOISELESS MEASUREMENTS

We repeat the idea of modified-CS for noiseless measurements in [11]. Consider the noiseless measurements’ case, i.e. (1) and assume that we have an exactly sparse signal sequence with slowly changing sparsity pattern (support). Let $T_t = \hat{N}_t$ denote an estimate of the support at t . At time, t , we have an estimate of the support from $t-1$, T_{t-1} . We would like to find a solution with the minimum number of new additions to T_{t-1} , that satisfies the data constraint. In other words, we would like to minimize the ℓ_0 norm of the solution along T_{t-1}^c (where c denotes complement of a set), i.e. solve

$$\hat{\beta} = \arg \min_{\beta} \|(\beta)_{T_{t-1}^c}\|_0, \text{ s.t. } y_t = A\beta \quad (3)$$

and then $\hat{x}_t = \hat{\beta}$ will be our solution (exact if enough measurements are available). But as discussed earlier, minimizing the ℓ_0 norm has

combinatorial complexity. So we propose to replace the ℓ_0 norm in (3) by the ℓ_1 norm as in Compressed Sensing [3, 7, 4] making the optimization problem convex and thus easy to solve. Thus at each time $t > 1$, we solve the following problem

$$\hat{\beta} = \arg \min_{\beta} \|(\beta)_{T_{t-1}^c}\|_1, \text{ s.t. } y_t = A\beta \quad (4)$$

and then set $\hat{x}_{t,ModCS} = \hat{\beta}$. The estimated support at t , T_t is computed as the indices of the elements of \hat{x}_t which are nonzero (in practice larger than a very small threshold), α_{nz} .

In [11], we showed that, for exact reconstruction, modified-CS needs at least $|T| + 2|\Delta|$ measurements, where T is the known part of the support (in this work, the support estimate from $t-1$) and $\Delta := N_t \setminus T$ is the unknown part. On the other hand, CS needs at least $2|T| + 2|\Delta|$ which is much larger when $|T| \gg |\Delta|$. We showed that exact reconstruction is possible with modified-CS if $\delta_{|T|+2|\Delta|} < 1/5$, while the similar result for CS requires $\delta_{3|T|+3|\Delta|} < 1/3$ [4]. Here δ_S is the S restricted isometry constant defined in [4].

In our implementation, at $t = 1$, we use enough observations, n , for exact reconstruction using CS. For $t > 1$, n is reduced to a much smaller number.

3. MODIFIED-CS-RESIDUAL FOR NOISY MEASUREMENTS

We have recaped modified-CS for noiseless measurements in the previous section as in [11], now we discuss a new algorithm to improve its performance for noisy measurements in this section.

When measurements are noisy, we relax the equality constraint of (4) using a modification of the LS-CS idea, but without using any prior model parameters. In this case, we at each time t , we solve

$$\hat{\beta} = \arg \min_{\beta} \gamma \|(\beta)_{T_{t-1}^c}\|_1 + \|\tilde{y}_{t,res} - A\beta\|_2^2$$

$$\hat{x}_{t,ModCS} = \hat{x}_{t,temp} + \hat{\beta} \quad (5)$$

where $\tilde{y}_{t,res} = y_t - A\hat{x}_{t,temp}$ and $(\hat{x}_{t,temp})_{T_{t-1}} = (\hat{x}_{t-1,NoisyModCS})_{T_{t-1}}$, $(\hat{x}_{t,temp})_{T_{t-1}^c} = 0$.

An important issue in the noisy measurements’ case is the following. While thresholding $\hat{x}_{t,ModCS}$ to estimate the support, T_t , is fairly accurate, the actual estimates in $\hat{x}_{t,ModCS}$ are not so accurate. Since our cost function in (5) does not have any term that penalizes large values of the estimate along T_{t-1} , the solver tries to add as much energy along T_{t-1} as possible (to keep the ℓ_2 error term small). Thus, the solution, $\hat{x}_{t,ModCS}$, is biased away from zero along T_{t-1} (“too large”) while it biased towards zero along T_{t-1}^c (“too small”), because of the ℓ_1 norm penalty. To remove this bias, we first estimate the support T_t and then compute a least squares (LS) estimate of $(x_t)_{T_t}$, while setting the estimate along T_t^c to zero, i.e.

$$(\hat{x}_{t,NoisyModCS})_{T_t} = A_{T_t}^\dagger y_t, \quad (\hat{x}_{t,NoisyModCS})_{T_t^c} = 0 \quad (6)$$

where $A_{T_t}^\dagger = (A_{T_t}' A_{T_t})^{-1} A_{T_t}'$ is the Moore-Penrose pseudo-inverse of A_{T_t} . Of course, some extra bias is also introduced due to false or missed additions in T_t , but this bias will be small if the addition threshold for computing additions to T_{t-1} is small. Computing a final LS estimate to reduce bias was first described in [5].

A second important issue is the following. As discussed above, the elements of $\hat{x}_{t,ModCS}$ along T_{t-1} will be larger than they should be. Thus, we perform the deletion of “near-zero” coefficients from T_t using the LS estimate, $\hat{x}_{t,NoisyModCS}$ and not using $\hat{x}_{t,ModCS}$. To introduce robustness (not delete a coefficient only because its estimate at the current time is small), we also use estimates from a few past time instants for deletion.

The complete algorithm is summarized in Algorithm 1.

4. IMPLEMENTATION FOR LARGE PROBLEMS

In the implementation, the memory problem is the difficult issue because we have to store each measurement matrices which is beyond

Algorithm 1 Modified-CS-residual for Noisy Measurements

Initialization: Do CS for x_0 using $\hat{x}_{0, NoisyModCS} = \arg \min_{\beta} \gamma \|\beta\|_1 + \|\tilde{y}_{t, res} - A\beta\|_2^2$.

Set $T_0 = \{i : |\hat{x}_{0, NoisyModCS, i}| \geq \alpha_{ini}\}$. For $t > 0$, do,

1. **Modified-CS-residual**

(a) Set $\hat{x}_{t, temp} = \hat{x}_{t-1, NoisyModCS}$ and compute $\tilde{y}_{t, res} = y_t - A\hat{x}_{t, temp}$.

(b) **Do Modified-CS-residual.** Compute $\hat{\beta} = \arg \min_{\beta} [\gamma \|(\beta)_{T_{t-1}^c}\|_1 + \|\tilde{y}_{t, res} - A\beta\|_2^2]$.

(c) **Compute additions to support.** Set $\hat{x}_{t, ModCS} = \hat{x}_{t, temp} + \hat{\beta}$ and compute $T_t = \{i : |\hat{x}_{t, ModCS, i}| > \alpha_a\}$.

2. **Least Square estimation using new support.** Set $(\hat{x}_{t, NoisyModCS})_{T_t} = A_{T_t}^\dagger y_t$, $(\hat{x}_{t, NoisyModCS})_{T_t^c} = 0$

3. **Deletion.** Compute the set $T_d = \{i : i \in T_t, \sum_{\tau=t-p+1}^t \hat{x}_{\tau, NoisyModCS, i}^2 < \alpha_d\}$ and update nonzero set $T_t \leftarrow T_t \setminus T_d$.

4. **Output** T_t and $\hat{x}_{t, NoisyModCS}$. Increment t and go to step 1.

most computers' memory. Hence, we have developed the computational efficient algorithms to handle the large data solving the memory problem for the application of MR imaging. This is similar to Candes' *ll magic code*[1] and we will post our codes on our website. Operators are defined to perform fast 2D DFT and DWT and then sample the measurements with regards to the sampling mask. Thus, what we need to store is only the sampling mask which eliminates the memory load. Primal-dual interior-point method with conjugate gradient search is used in noiseless case and gradient descent method is used in noisy case. In both cases, operators are used instead of matrix operation.

The operators we used are based on four basic operators $A(\beta)$, $A'(y)$ and $A_T(\beta)$, $A_T'(y)$. Thus, we implement $A(\beta)$ in three steps.

1. Compute 2D inverse DWT of β to obtain x
2. Apply fast 2D DFT to x to obtain y_{full}
3. Use sampling mask M to extract the Fourier coefficients. This gives y_{samp} . Split the real part and imaginary part of y_{samp} to form a new real vector $y = [Re(y_{samp}) \quad Im(y_{samp})]$. Then this new vector is the output, $A(\beta)$.

The operator, $A_T(\beta_T)$ is implemented as $A(\tilde{\beta})$ with $\tilde{\beta}_T = \beta_T$ and $\tilde{\beta}_{T^c} = 0$.

We implement $A'(y)$ in a reverse fashion as follows.

1. Generate a zeros vector y_{full} of size m . Split y into halves y_{re} and y_{im} . Construct a new complex vector by doing $y_{samp} = y_{re} + i \cdot y_{im}$. Set nonzero mask locations of y_{full} equal to y_{samp} .
2. Apply inverse fast 2D DFT on y_{full} to obtain x .
3. Do 2D DWT on x to obtain the final output $A'(y)$.

To implement $A_T'(y)$ is just to extract the coefficients in the set T after applying A' to y . With these function handles, we are able to implement all steps of primal-dual interior point methods. By doing these, we no longer depend on the matrices forms of all operation, but we can solve the problem in a both memory and computationally efficient method. Storage requirement is now only $O(m)$ to store the sampling mask, or the reconstructed signals, instead of $O(mn)$ to store the entire A . Typically, $n \sim 0.2m$ so this is quite large. Time complexity reduces from $O(m^3)$ (to implement 1D matrix version of DFT) to $O(\sqrt{m} \log m)$ (to implement 2D version of FFT). The reconstruction of a 64×64 image may take 6 minutes for 1D matrix version while 2D operator version only costs 1 minute.

5. EXPERIMENTAL RESULTS

In this section, we implement our algorithms on three real data sequences: a cardiac dynamic sequence, a larynx sequence and a brain sequence. The sparsified cardiac sequence(created by setting small wavelet coefficients to zero and computed inverse DWT) is strictly sparse and its support with the coefficients changes slowly. The actual(not sparsified) cardiac sequence and larynx sequence are not sparse but compressible and both have slowly changing trend on large nonzero coefficients and corresponding sets.

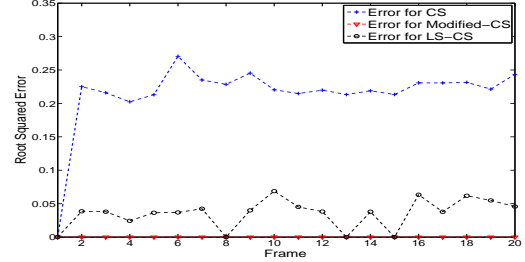


Fig. 2. Noiseless measurements, Sparsified cardiac. Comparing Modified-CS with CS and LS-CS. CS reconstruction obviously fails and LS-CS can not exactly reconstruct the sequence. Support size, $|N_t| \approx 10\%$ of m . $n = 18\%$ observations were used for $t > 1$, while using $n = 50\%$ observations at $t=1$ (use CS at $t=1$).

The larynx sequence, with size 256×256 , and the brain sequence, with size 64×64 , are both compressible in wavelet domain. The number of large coefficients which conserve 99% of the total energy $|N_t| \approx 600$ (about 15%) for brain sequence and $|N_t| \approx 4600$ (about 7%) for larynx sequence. For all experiments, at $t=1$, we perform simple CS and use $n = 50\%$ observations.

We compare the performance of CS and our modified-CS algorithm for noiseless measurement as described in sec. 2. Root squared error defined by $e(t) = \|x_t - \hat{x}_t\|_2 / \|x_t\|_2$ is used to compare the reconstruction performance for noiseless measurement algorithms.

Fig. 2 is the comparison of reconstruction for CS, LS-CS and our algorithm on sparsified image sequence and the comparison of original sequence with reconstructed sequences using these methods. For the $t > 1$ frames, observations are reduced to 16% for Fourier measurement. Under such a small number of observations, CS algorithm definitely fails, but from Fig. 2 we can see our algorithm still can reconstruct the sequence exactly. To exactly reconstruct the sequence, CS algorithm requires 35% observations while our Modified-CS algorithm only needs 16%. This greatly reduces the sequence acquisition and reconstruction time. Also, LS-CS fails to reconstruct the sequence exactly. We give the error comparison for the actual cardiac sequence in Fig. 3(left plot).

Next, we apply our algorithm to the 256×256 larynx sequence. For this compressible image sequence, we use 16% observations for $t > 1$ frames. As is shown in Fig. 3(right plot) and 4, we can still reconstruct the sequence with small error which is $2\% \sim 3\%$. Also, of course CS and LS-CS reconstruction have large error.

We compare the performance of our Modified-CS-residual algorithm for noisy measurement with BPDN and BPDN-LS algorithms. For noisy measurement, we use signal to noise ratio(SNR) to denote the level of noise where $SNR = 20 \log \frac{\|Ax_t\|_2}{\|y_t - Ax_t\|_2}$. Root mean squared error(RMSE) is used to compare the reconstruction performance for noisy measurement algorithm and 50 times Monte Carlo simulations are done for computing RMSE. We test for $SNR \approx$

40db. We pick γ as the same in [2]: $\gamma = 4\sqrt{2\log m}$.

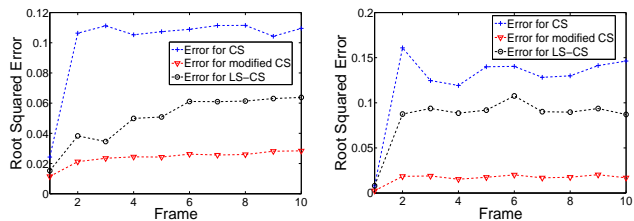


Fig. 3. Noiseless measurements, cardiac sequence (left plot), larynx sequence (right plot). Comparing modified-CS with CS and LS-CS. Image size, $m = 256 \times 256$. 99% energy support, $|N_t| \approx 7\%$ of m . $n = 16\%$ observations were used for $t > 1$.

We show in Fig.5(bottom figure) visually the two reconstructed sequences using Modified-CS-residual and BPDN [9] for the first 4 frames of the noisy brain sequence with 25% observations for $t > 1$ frames. We can see that BPDN reconstructed sequence is blurred, but Modified-CS-residual reconstructed sequence can clearly display the brain lobes and thus Modified-CS-residual algorithm is able to recover more detailed information such as edges than BPDN. We also give the RMSE comparison in Fig.5(top figure) comparing Modified-CS-residual with BPDN, BPDN-LS and LS-CS. We do not show the reconstruction of BPDN-LS and LS-CS since they have similar performance with BPDN and Modified-CS-residual separately. Although the brain sequence is not very sparse, our algorithm still bears better performance and produces good reconstruction.

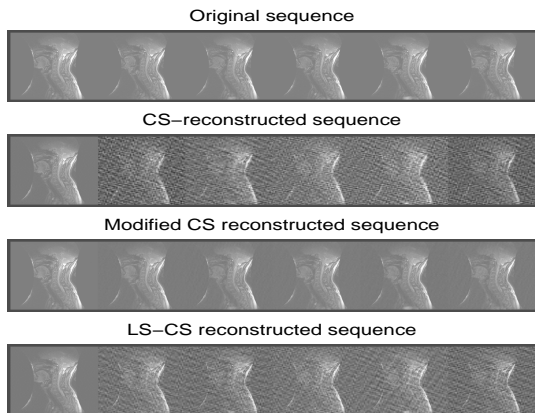


Fig. 4. Noiseless measurements, True larynx Sequence. Reconstruction of CS, LS-CS and Modified-CS. CS reconstruction is obviously quite noisy. Image size, $m = 256 \times 256$. 99% energy support, $|N_t| \approx 7\%$ of m . $n = 16\%$ observations were used for $t > 1$.

6. CONCLUSIONS AND FUTURE WORK

We studied the problem of recursively and causally reconstructing a sequence of natural images from a reduced number of linear projection measurements taken in a domain that is “incoherent” with respect to the image’s sparsity basis. Most existing solutions are either offline and non-causal or cannot compute an exact reconstruction (for truly sparse signal sequences), except using as many measurements as those needed for CS. The key idea of our solution is to design a modification of CS when a part of the support set is known (available from reconstructing the previous image). We demonstrated the exact reconstruction property of our solution on real image sequences (dynamic MR imaging of cardiac larynx and brain sequences), using much fewer measurements than those required for CS. Small error reconstruction is achieved for approximately sparse signals or noisy measurements.

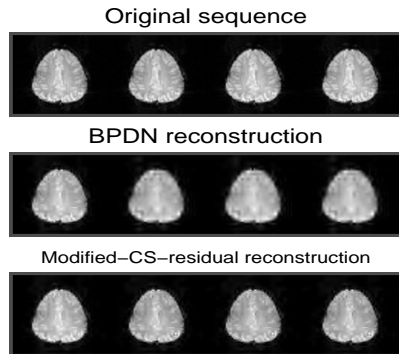
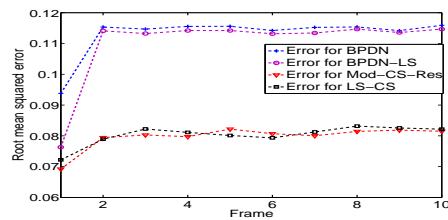


Fig. 5. Noisy measurements, Brain Sequence. Top: RMSE of Modified-CS-residual with BPDN, BPDN-LS and LS-CS for 64×64 brain sequence. Bottom: Reconstruction of BPDN&Modified-CS-residual. $|N_t| \approx 15\%m$. $n = 25\%m$ used for $t > 1$. $SNR \approx 40db$

7. REFERENCES

- [1] E. Candes and J. Romberg. 11-magic: A collection of matlab routines for solving the convex optimization programs central to compressive sampling. Available: www.acm.caltech.edu/11magic.
- [2] E. Candès and Y. Plan. Near-ideal model selection by l_1 minimization. *Preprint*, 2007.
- [3] E. Candes, J. Romberg, and T. Tao. Robust uncertainty principles: Exact signal reconstruction from highly incomplete frequency information. *IEEE Trans. Info. Th.*, 52(2):489–509, 2006.
- [4] E. Candes and T. Tao. Decoding by linear programming. *IEEE Trans. Info. Th.*, 51(12):4203 – 4215, Dec. 2005.
- [5] E. Candes and T. Tao. The dantzig selector: statistical estimation when p is much larger than n . *Annals of Statistics*, 2006.
- [6] V. Cevher, A. Sankaranarayanan, M. Duarte, D. Reddy, R. Baraniuk, and R. Chellappa. Compressive sensing for background subtraction. In *ECCV*, 2008.
- [7] D. Donoho. Compressed sensing. *IEEE Trans. on Information Theory*, 52(4):1289–1306, April 2006.
- [8] H. Jung, J. C. Ye, and E. Y. Kim. Improved k-t blask and k-t sense using focuss. *Phys. Med. Biol.*, 52:3201 – 3226, 2007.
- [9] M. Lustig, D. Donoho, and J. M. Pauly. Sparse mri: The application of compressed sensing for rapid mr imaging. *Magnetic Resonance in Medicine*, 58(6):1182–1195, December 2007.
- [10] A. Martin, O. Weber, D. Saloner, R. Higashida, M. Wilson, M. Saeed, and C. Higgins. Application of MR Technology to Endovascular Interventions in an XMR Suite. *Medica Mundi*, 2002.
- [11] N. Vaswani and W. Lu. Modified-cs: modifying compressive sensing for problems with partially known support. In *ISIT*, 2009.
- [12] C. Qiu, W. Lu, and N. Vaswani. Real-time dynamic mr image reconstruction using kalman filtered cs. In *ICASSP*, 2009.
- [13] C. Rozell, D. Johnson, R. Baraniuk, and B. Olshausen. Locally competitive algorithms for sparse approximation. In *ICIP*, 2007.
- [14] N. Vaswani. Analyzing least squares and kalman filtered compressed sensing. In *ICASSP*, 2009.